

12-16-2021

## Prediction of E.M.F. Variation due to Shifting the Resultant Field in DWR Synchronous Generator.

Hassan Abou-Tabl

*Electrical Power & Machines Department., Faculty of Engineering., El-Mansoura University., Mansoura., Egypt.*

Follow this and additional works at: <https://mej.researchcommons.org/home>

---

### Recommended Citation

Abou-Tabl, Hassan (2021) "Prediction of E.M.F. Variation due to Shifting the Resultant Field in DWR Synchronous Generator." *Mansoura Engineering Journal*: Vol. 4 : Iss. 2 , Article 4.

Available at: <https://doi.org/10.21608/bfemu.2021.187358>

This Original Study is brought to you for free and open access by Mansoura Engineering Journal. It has been accepted for inclusion in Mansoura Engineering Journal by an authorized editor of Mansoura Engineering Journal. For more information, please contact [mej@mans.edu.eg](mailto:mej@mans.edu.eg).

PREDICTION OF E.M.F. VARIATION DUE TO SHIFTING  
THE RESULTANT FIELD IN DWR SYNCHRONOUS GENERATOR

BY

Dr. Eng. Hassan Ali Abou-Tabl\*

**ABSTRACT:**  
-----

In this paper the e.m.f. equation of an idealised synchronous generator, having a divided-winding-rotor, is derived. The equation is obtained in two alternative forms whereby the effect of shifting the resultant field around the rotor on the sinusoidal induced e.m.f. can be approached. Shifting the resultant field axis from its original direction results actually in considerable distortion in the resultant no-load m.m.f. distribution. This distortion affects the induced e.m.f., as exhibited by the measured values on machine model. A comparative study of the results, obtained by applying the method of harmonic analysis to the different m.m.f. waveforms, leads to the interpretation of the variation in the measured e.m.f. Away from this method, however, a reliable measure is suggested for a quick prediction of this e.m.f. variation.

**O. Nomenclature:**

- $E_c$  : = induced e.m.f. per phase of c.w.r. synchronous generator, (r.m.s.);
- $E_R$  : = induced e.m.f. per phase of d.w.r. synchronous generator, (r.m.s.);
- $E_a$  : = induced e.m.f. per phase due to  $F_a$ , sinusoidal r.m.s.;
- $E_r$  : = induced e.m.f. per phase due to  $F_r$ , sinusoidal r.m.s.;
- $E$  : = no-load voltage per phase of d.w.r. synchronous generator (r.m.s.);
- $\bar{V}_{ao}$  : = no-load voltage per phase "a" of a d.w.r. synchronous generator, vector form;
- $F_c$  : = m.m.f. per pole, sinusoidal peak;
- $F_{Rc}$  : = resultant peak of d.w.r., sinusoidal;
- $F_{Rc}$  : = resultant of  $F_R$ , sinusoidal peak;
- $F_{Rc}$  : = resultant of  $F_R$ , sinusoidal peak;
- $F_{Rc}$  : = m.m.f., nonsinusoidal;
- $I_f$  : = field excitation current, sinusoidal peak;
- $I_{fd}$  : = field excitation current, sinusoidal;
- $I_{fd}$  : = current in either field winding voltage, sinusoidal peak;
- $I_{fd}$  : = currents in a-r axes;
- $I_{fd}$  : = currents in d-q axes;

Mansoura University,

$(C_f)_i$	: = field-currents transformation;
$(C_f)_v$	: = field-voltages transformation;
$(V_o)_{dq}$	: = matrix of steady state, no-load armature voltages in d-q axes;
$T_{ph}$	: = number of turns per phase;
$K_{wl}$	: = winding-factor, fundamental;
$D$	: = inner diameter of stator, m.;
$L$	: = core-length, m.;
$l_g$	: = air-gap length, m.;
$P$	: = number of poles;
$\Phi_c$	: = conventional flux per pole, weber;
$\mu_0$	: = free space permeability = $4\pi/10^7$ henry per m.;
$\tau$	: = pole-winding spread;
$\alpha$	: = $\beta/2$ where $2\beta$ : = pole-arc;
$\theta'$	: = shift-angle measured from the 180°-active axis;
$\theta_v$	: = shift-angle of $\bar{V}_{ao}$ w.r.t. the d-axis;
$\theta_f$	: = shift-angle of $F_R$ w.r.t. the d-axis;
$\omega$	: = angular speed, synchronous in electrical radians/sec.;
c.w.r.	: = conventional-winding-rotor;
d.w.r.	: = divided-winding-rotor;

## 1. INTRODUCTION:

The idealised d.w.r. synchronous generator assumes a sinusoidal distribution of each of the resultant field and its components at no-load. The peaks of both components,  $F_a$  and  $F_r$ , can be adjusted such that the resultant peak  $F_R$  is held constant while it is shifted around the rotor<sup>1</sup>. Based on this assumption, an equation of the induced e.m.f. per phase can be derived. In this paper the principle of superposition is applied to obtain this e.m.f. equation in a classical form. Also, an equivalent model in the d-q axes is used to obtain the e.m.f. equation as an alternative method. In this case, an additional transformation is required to transform the field circuit, in the active-and reactive-axis, into its equivalent in the d-q axes. Both e.m.f. equations help predicting the effect of the shift-angle  $\theta'$  on the sinusoidal induced e.m.f. per phase. For the purpose of comparison, the equation of the sinusoidal induced e.m.f. of the c.w.r. synchronous generator is presented first.

In an actual d.w.r. synchronous generator, shifting the resultant field axis from its original direction along the d-axis results in a considerable distortion in the resultant no-load m.m.f. distribution<sup>2</sup>. This distortion includes the shape as well as the absolute maximum value, and also affects the induced e.m.f.<sup>1</sup> The prediction of the e.m.f. variation with the shift-angle is visualised by a comparative study of the results obtained by applying the harmonic analysis method to the corresponding m.m.f. waveforms.

**2. C.W.R. Synchronous Generator, The E.M.F. Equation:**

The derivation of the e.m.f. equation of a c.w.r. synchronous generator is based on the assumption of sinusoidal field distribution in the air-gap<sup>4</sup>. This equation has the well known form:

$$E_c = (2 \pi / \sqrt{2}) K_{wl} f \Phi_c T_{ph}$$

or

$$E_c = 4.44 K_{wl} f \Phi_c T_{ph} \dots\dots\dots(1)$$

The sinusoidal flux per pole  $\Phi_c$  may be obtained by

$$\begin{aligned} \Phi_c &= (\text{M.M.F.})(\text{permeance}) \\ &= (2 / \pi) F_c \Lambda \dots\dots\dots(2) \end{aligned}$$

Where  $\Lambda$  : = permeance of magnetic path which is mainly the air-gap length;

$$\begin{aligned} &= \mu_o \cdot \text{area} / l_g \\ &= \mu_o (\pi D L/P) / l_g, \quad \text{webers/AT} \\ &= \text{constant.} \end{aligned}$$

Substituting for  $\Phi_c$  from eqn.(2) into eqn.(1) gives

$$E_c = 4.44 K_{wl} f T_{ph} (2/\pi) \Lambda F_c$$

or

$$E_c = K F_c \dots\dots\dots(3)$$

where  $K$  : = constant

$$= 4.44 K_{wl} f T_{ph} (2/\pi) \Lambda, \text{ volt/AT} \dots\dots\dots(4)$$

Equation(3) assumes, for linear conditions, that the e.m.f. induced per phase is directly proportional to the maximum sinusoidal m.m.f.

**3. D.W.R. Synchronous Generator, Sinusoidally Induced E.M.F.:**

In the following, two alternative methods are applied to obtain the sinusoidal induced e.m.f. per phase of a d.w.r. synchronous generator. Both methods consider an ideal machine in which saturation is neglected and the resultant no-load m.m.f. distribution is assumed to be sinusoidal. However, the first method applies the principle of superposition while the second makes use of an equivalent model in the d-q axes. Results are discussed to have an idea about the effect of the shift-angle on the sinusoidal induced e.m.f.

**3.1. E.M.F. Equation Based ON The Principle of Superposition:**

With respect to its field-winding, a synchronous generator with a divided-winding-rotor may be considered as a c.w.r. synchronous generator having two field-windings, namely, the active-and reactive-field winding.

Either winding has the same number of poles, but their magnetic axes are displaced from each other<sup>1</sup> by an angle  $\tau/2$ . Both field windings are mounted on the rotor and the corresponding fields,  $F_a$  and  $F_r$ , link the 3-phase armature winding at the same speed.

In order to derive an equation for the sinusoidal induced e.m.f. either field ( $F_a$  or  $F_r$ ) is assumed to act individually. Accordingly, the principle of superposition in its classical form can be applied to get the induced e.m.f. per phase. Each sinusoidal field component,  $F_a$  and  $F_r$ , creates a corresponding e.m.f. component,  $E_a$  and  $E_r$  respectively, in the same phase-winding.

According to equation (3), both e.m.f. components can be given as:

$$E_a = K F_a \dots\dots\dots(5.1)$$

and

$$E_r = K F_r \dots\dots\dots(5.2)$$

The use of the same constant  $K$  as given by eqn.(4), takes into account the assumption that both fields have the same reluctance (assuming a cylindrical rotor). Both fields are expressed<sup>1</sup> in terms of the resultant field  $F_R$ , and the two e.m.f. components can be given as

$$E_a = K C_a F_R \dots\dots\dots(6.1)$$

and

$$E_r = K C_r F_R \dots\dots\dots(6.2)$$

where  $C_a$  and  $C_r$  are the no-load field control factors:

$$C_a = \cos(\theta' + \alpha) / \cos 2\alpha \dots\dots\dots(7.1)$$

and

$$C_r = \sin(\theta' - \alpha) / \cos 2\alpha \dots\dots\dots(7.2)$$

As the m.m.f. components are displaced by  $\tau/2$  from each other, both e.m.f. components will be displaced by the same phase-angle  $\tau/2$ , Fig. 1. They may be of different magnitudes according to the shift-angle  $\theta'$  of the resultant field  $F_R$ . Referring to Fig. 1, a relation for the resultant (total) induced e.m.f. can be written as:

$$E_R^2 = E_a^2 + E_r^2 + 2 E_a E_r \cos(\tau/2)$$

Substituting for  $E_a$  and  $E_r$  from eqs. (6), then

$$E_R^2 = K^2 F_R^2 [C_a^2 + C_r^2 + 2 C_a C_r \cos(\tau/2)]$$

As long as  $F_a$  and  $F_r$  are the sinusoidal components of the resultant  $F_R$ , the term between brackets is equal to unity. Consequently, the sinusoidal induced e.m.f. per phase of a d.w.r. synchronous generator is

$$E_R = K F_R \dots\dots\dots(8)$$

Equation (8) has the same form as that derived for the conventionally induced e.m.f., eqn.(3).

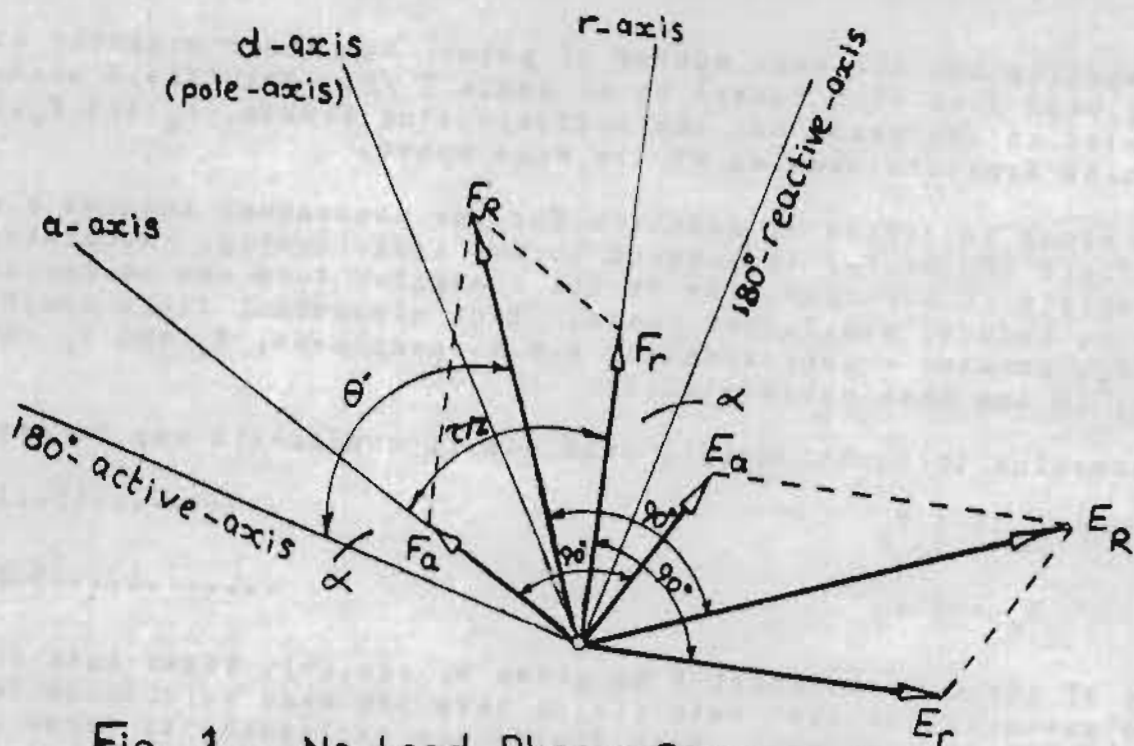


Fig. 1 No-Load Phasor Diagram of a D.W.R. Synchronous Generator.

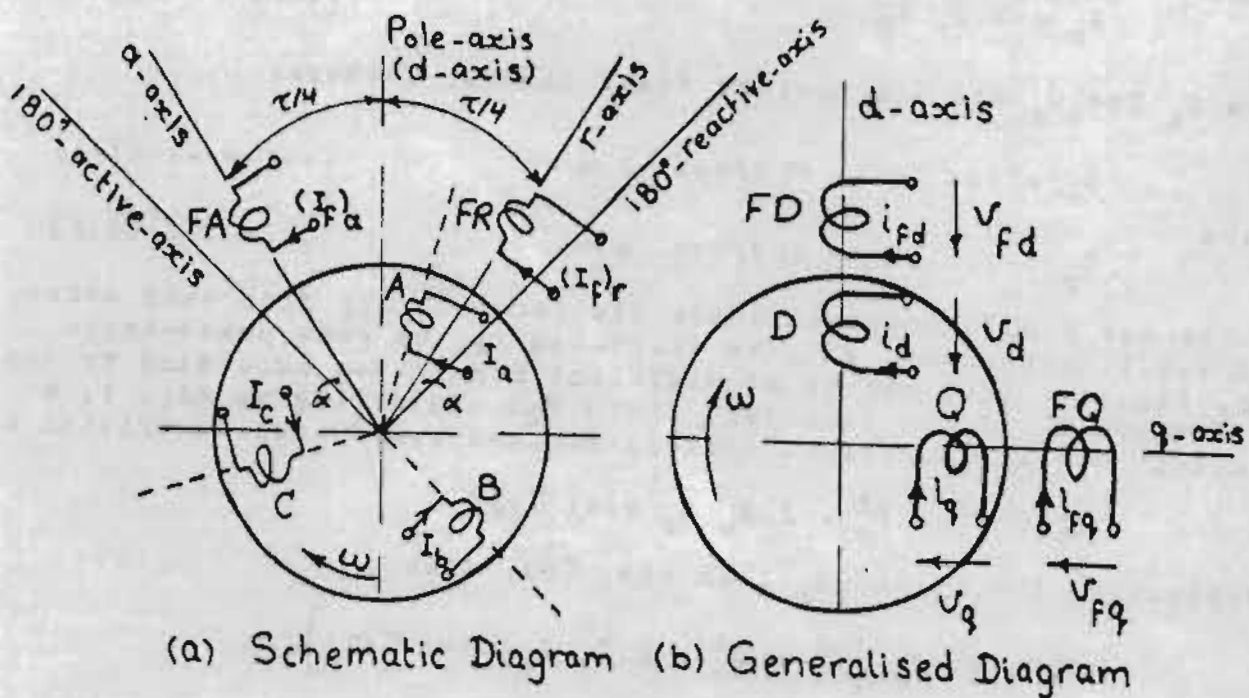


Fig.2 2-Pole D.W.R. Synchronous Generator  
(without damper-winding)

**3.2. E.M.F. Equation based on an Equivalent Model:**

Fig. 2 gives a schematic diagram of a 2-pole d.w.r. synchronous generator and its equivalent model in the d-q axes. The field axes, a-r, in the idealised machine are equally displaced about the pole-axis. They are displaced from each other by an angle equal to  $\tau/2$ . The armature winding is the same three-phase balanced winding as that of a c.w.r. synchronous generator. Parks transformation<sup>3,5</sup> can be used to transform the rotating axes (a,b,c) to the stationary axes (d,q,0).

**3.2.1. Dual-Field Transformation:**

In a conventional machine the stationary field axis is considered to be along the d-axis, therefore no transformation is needed. However, in a synchronous machine with a d.w.r., an additional transformation is required to transform the dual field winding in the a-r axes to its equivalent in the d-q axes.

For a divided-winding-rotor with  $\tau < 180^\circ$ , the field current and voltage-transformations,  $(\underline{C}_f)_i$  and  $(\underline{C}_f)_v$  respectively, are not identical. The field current transformation is

$$(\underline{C}_f)_i = \begin{bmatrix} \cos(\tau/4) & \cos(\tau/4) \\ -\sin(\tau/4) & \sin(\tau/4) \end{bmatrix} \dots(9)$$

This transformation ensures that the resultant field due to the equivalent excitation in the d-q axes still retains its original magnitude and direction. The shift-angle of the resultant field w.r.t. the d-axis is given by

$$\theta_f = \theta' - (\pi/4) \dots\dots\dots(10)$$

In order to keep the excitation power invariable,  $(\underline{C}_f)_v$  is chosen such that

$$(\underline{C}_f)_v = (\underline{C}_f)_i^{-1}$$

For a divided-winding-rotor with  $\tau = 180^\circ$ , the a-r axes are perpendicular and equally displaced about the d-axis thus

$$(\underline{C}_f)_i = (\underline{C}_f)_v = (\underline{C}_f)$$

where

$$(\underline{C}_f) = \begin{bmatrix} \cos(\pi/4) & \sin(\pi/4) \\ -\sin(\pi/4) & \cos(\pi/4) \end{bmatrix} \dots\dots\dots(11)$$

3.2.2. Steady-State No-Load Voltages  $(\underline{V}_o)_{dq}$ :

The voltage equations are first written for the generalised diagram, Fig. 2-b, and then simplified under the no-load conditions ( $i_d = i_q = 0$ ) to get the steady state no-load voltages. Thus

$$\begin{bmatrix} V_{do} \\ V_{qo} \end{bmatrix} = \begin{bmatrix} 0 & \omega M_q \\ -\omega M_d & 0 \end{bmatrix} \cdot \begin{bmatrix} I_{fd} \\ I_{fq} \end{bmatrix}$$

or  $(\underline{V}_o)_{dq} = (\underline{M}) (\underline{I}_f)_{dq} \dots\dots\dots(12)$

$(\underline{I}_f)_{dq}$  is given in terms of the actual excitation currents as

$$(\underline{I}_f)_{dq} = (\underline{C}_f)_i (\underline{I}_f)_{ar} \dots\dots\dots(13.1)$$

where  $(\underline{I}_f)_{ar} = \begin{bmatrix} (I_f)_a \\ (I_f)_r \end{bmatrix} = \begin{bmatrix} C_a \\ C_r \end{bmatrix} (I_f)_{d.w.} \dots\dots\dots(13.2)$

as given in Ref. 1. Therefore, the no-load steady state armature voltages in the d-q axes are,

$$V_{do} = -\omega M_q (I_f)_{d.w.} \sin(\tau/4)(C_a - C_r) \dots\dots(14.1)$$

and  $V_{qo} = -\omega M_d (I_f)_{d.w.} \cos(\tau/4)(C_a + C_r) \dots\dots(14.2)$

3.2.3. No-load Voltage per phase:

Taking phase "a" only into consideration and assuming that its axis coincides with the d-axis, the retransformation from the (d,q,0) axes to the (a,b,c) axes gives the no-load voltage per phase as

$$V_{ao} = V_{do} \cos \omega t - V_{qo} \sin \omega t \dots\dots\dots(15)$$

which can be written in complex form as

$$\bar{V}_{ao} = (V_{do} + j V_{qo}) / \sqrt{2} \dots\dots\dots(16)$$



Substituting for  $V_{d0}$  and  $V_{q0}$  from eqn.(14) and assuming that  $M_d = M_q = M$ , the absolute no-load voltage(r.m.s.) becomes

$$|V_{a0}| = (1/\sqrt{2}) \omega M(I_f)_{d.w.} \sqrt{[C_a^2 + C_r^2 + 2C_a C_r \cos(\tau/2)]}$$

The term under the square root is equal to unity as stated before.  $\bar{V}_{a0}$  can then be represented by

$$\bar{V}_{a0} = E \angle \theta_v \dots\dots\dots(17)$$

where  $E = (1/\sqrt{2}) \omega M(I_f)_{d.w.} \dots\dots\dots(18)$

and  $\theta_v = \theta' + (\pi/4) \dots\dots\dots(19)$

is the phase-shift of  $\bar{V}_{a0}$  w.r.t. the d-axis. Equation (18) is an alternative form for the e.m.f. equation of a d.w.r. synchronous generator. This induced e.m.f. lags the resultant field by an angle equal to  $90^\circ$ ; where  $\theta_v - \theta_f = \pi/2$ .

**3.3. Shift-Angle Effect on the Sinusoidal Induced E.M.F.:**

It is now obvious from equations (8) and (18) that the sinusoidal induced e.m.f. per phase of a d.w.r. synchronous generator is not affected by shifting the resultant field around the rotor. Equation (8) shows that the induced e.m.f. remains constant so long as  $F_R$  is constant.

The no-load voltage given by eqn.(18) is the induced e.m.f. per phase according to the excitation current  $(I_f)_{d.w.}$

when supplied to either the active or reactive field winding. For dual excitation, however, as long as both excitation currents,  $(I_f)_a$  and  $(I_f)_r$ , are related to  $(I_f)_{d.w.}$  to keep  $F_R$  constant, the induced e.m.f.  $E$  at any shift-angle  $\theta'$  of the resultant field will remain also constant. It is preferable to have the resultant field axis along the d-axis. In this case, both excitation currents will be equal and both field windings will be loaded equally.

**4. M.M.F. Harmonic-Study Leading to the E.M.F. Variation:**

In Ref. 2, a detailed study is carried out on the m.m.f. distributions established in the air-gap of a d.w.r. synchronous generator while the resultant field axis is shifted around the rotor. The results show that the no-load m.m.f. distribution does not remain constant as the shift angle is varied.

Here arises the question about the effect of m.m.f. variation on the induced e.m.f. The assumption that the fundamental m.m.f. approximates the actual m.m.f. distribution and that it is quite enough to derive the sinusoidal e.m.f. equation, needs to be checked again.

A reliable tool to judge this subject is to use the Fourier Series to obtain the harmonic content of the different resultant

Table (1)

Shift Angle $\theta'$ , $\tau =$	Harmonic Peak Ratio														
	$h_1$			$h_3$			$h_5$			$h_7$			$h_9$		
	180°	150°	120°	180°	150°	120°	180°	150°	120°	180°	150°	120°	180°	150°	120°
45°	.819	.945	1.059	.094	.080	0.00	.039	.010	.049	.022	.007	.029	.013	.014	0.00
60°	.785	.901	1.009	.091	.095	.121	.032	.014	.047	.023	.021	.030	.012	.010	.022
75°	.872	1.007	1.223	.104	.155	.285	.036	.011	.056	.021	.038	.033	.019	.016	.049
82.5°	.956	1.099	.929	.109	.194	.261	.041	.011	.041	.024	.048	.026	.020	.014	.046
90°	1.154	.941	.797	.137	.189	.264	.051	.010	.038	.031	.050	.020	.022	.015	.044
105°	.872	.771	.705	.104	.184	.285	.036	.004	.035	.021	.046	.018	.019	.008	.049
120°	.785	.697	.583	.091	.175	.265	.032	.007	.029	.023	.049	.013	.012	.005	.042
135°	.819	.725	.611	.094	.194	.285	.039	.002	.028	.022	.052	.017	.013	.006	.049

Table (2)

$\theta'$	$\tau = 180^\circ$		$\tau = 150^\circ$		$\tau = 120^\circ$	
	$(a_1/a)$	A	$(a_1/a)$	A	$(a_1/a)$	A
45°	1.040	.943	1.031	.929	1.011	.923
60°	.930	.978	.918	.961	.898	.957
75°	.912	.994	.884	.999	.934	1.000
82.5°	.913	.998	.884	1.000	.862	1.003
90°	.980	1.000	.862	1.020	.850	.979
105°	.912	.994	.095	.990	.948	.984
120°	.930	.978	.954	.932	.937	.917
135°	1.040	.943	1.108	.864	1.167	.800

m.m.f. waveforms. A computer-aided harmonic analysis study is carried out for the summarised groups of waveforms obtained in Ref. 2. Harmonic-peak ratios  $h_n$  are listed in Table (1) with the different shift-angle  $\theta'$ . In the following, the two ordinary criteria, which make use of these ratios, are discussed. They are usually used for judging the equivalence of the fundamental to the corresponding actual m.m.f. distribution.

#### 4.1. Creterion (1): The Fundamental Peak Ratio $h_1$

The fundamental peak ratio  $h_1$  relates the fundamental peak of the resultant m.m.f. distribution to its absolute maximum  $(F_R)_{max}$ . This ratio is plotted against  $\theta'$  in Fig. 3 for a complete revolution of the resultant field-axis around the air-gap.

The plotting shows how this ratio is affected by the shift-angle  $\theta'$ , as well as by the pole winding spread  $\tau$ . But when the absolute values of the fundamental peaks are calculated they seem to be approximately constant for a given  $\tau$ .

This result can be interpreted by having a look at Figs. 3 and 4. It is seen, for a given  $\tau$ , that the variation of  $h_1$  is compensated by a counter variation of the maximum resultant  $(F_R)_{max}$ . If a maximum variation of 0.08 p.u. in the absolute fundamental peak is tolerated, then it may be assumed constant.

#### 4.2. Creterion (2): The Ratio of Fundamental Area ( $a_1/a$ )

This ratio relates the fundamental half-wave area to the corresponding resultant m.m.f. half-wave area. It gives an indication of how much is the sinusoidal flux per pole compared with the actual flux per pole. This  $a_1/a$  ratio is calculated for the different m.m.f. waveforms and the results obtained are listed against  $\theta'$  in Table (2).

Usually, the variation in  $(a_1/a)$  is also taken to give an indication about the probable variation in the induced e.m.f. This convention does not give the whole truth in case of a d.w.r. For example: for  $\tau = 120^\circ$  the ratio  $(a_1/a)$  has a maximum value when the resultant field axis is along the q-axis, while the measured e.m.f., Fig. 6, shows a minimum value at the same shift-angle.

### 5. Prediction of E.M.F. Variation due to Shift-angle:

The variation in the induced e.m.f. with varying  $\theta'$ , can not be predicted by observing the variation in  $h_1$ , or the variation in  $(a_1/a)$  alone. While the variation of the first ratio seems to be constant, the second ratio fails to evaluate the e.m.f. variation. Therefore, effects of higher harmonics must be taken into consideration when the method of harmonic analysis is used to evaluate the e.m.f. variation. For this reason a third criterion, which is related mainly to the higher harmonics, must be introduced.

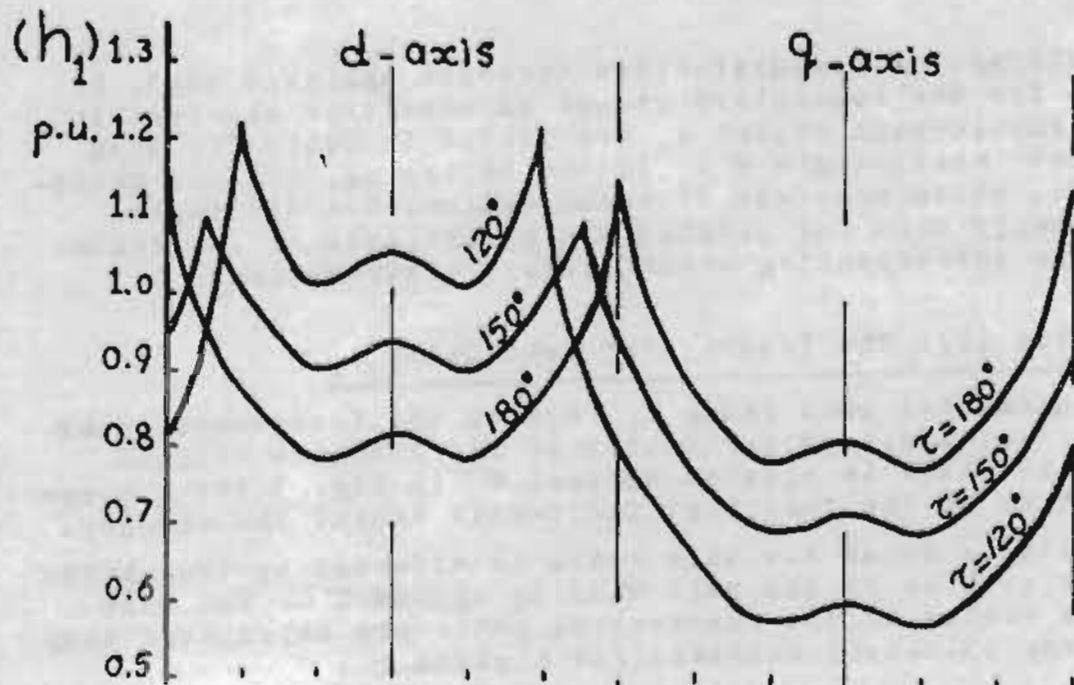


Fig. 3 Fundamental Peak Ratio

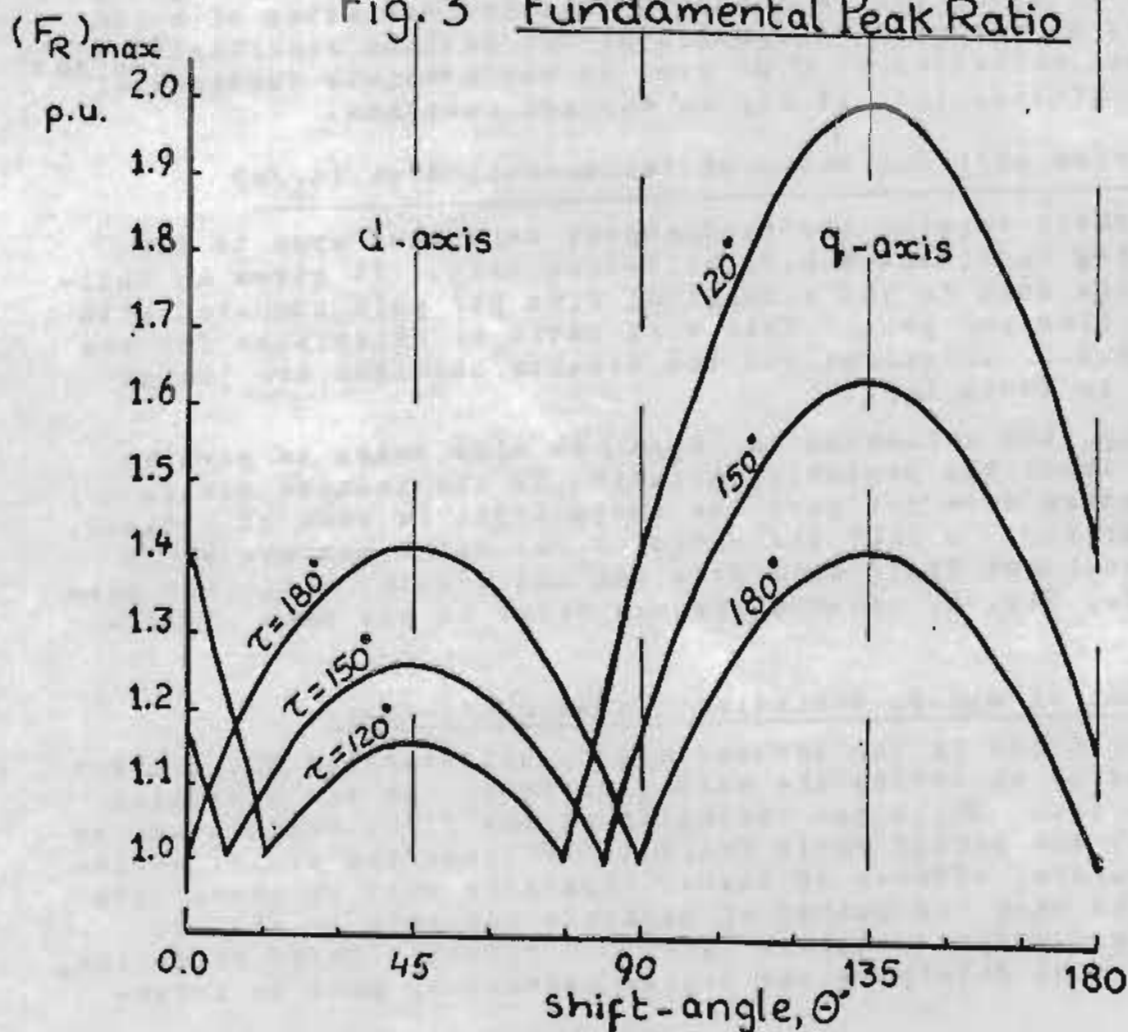


Fig. 4 Relative Maximum M.M.F.

### 5.1. Creterion (3): The Relative Harmonic Ratio ( $H_n$ ):

This creterion is introduced to have a comprehensive approach to the effect of the shift-angle on the resultant m.m.f. and in turn, on the induced e.m.f. It relates the nth harmonic peak of a resultant m.m.f. distribution to the corresponding hermonic peak of the mono-acting distribution by

$$H_n = (F_n)/(F_n)_o \quad \dots\dots\dots(20)$$

The mono-acting distribution is that m.m.f. distribution of the active-or reactive-field winding when either of them is acting alone to get the rated no-load voltage.

The variation of the ratio ( $H_n$ ) with  $\theta'$  gives the variation effect of the corresponding harmonic on the resultant air-gap m.m.f. Accordingly, it can be taken as a measure of the expected variation in the induced e.m.f. Calculated values of ( $H_n$ ) for harmonics higher than the third show a very small effect, which is approximately constant and so small that it can be neglected.

The relative ratios of the 1st and 3rd harmonics are given in Figs. 7 and 8 respectively. It is seen that the variation in  $H_1$  is within 8% and may assumed to be constant. On the other hand, the relative ratio of the third harmonic,  $H_3$ , exhibits a considerable variation.

For  $\tau = 180^\circ$ , the variation of  $H_3$  appears to be constant. For  $\tau < 180^\circ$ , it has a decreasing effect in the d-axis region and an increasing effect in the q-axis region. Fig.8 also shows that a minimum and a maximum value of  $H_3$  occurs exactly at the d- and q-axis respectively. While this minimum value is equal to zero for  $\tau = 120^\circ$ , the corresponding maximum value is equal to 2.0 per-unit.

### 5.2. Shift-angle Effect on the Measured E.M.F.:

The three creteria mentioned above are helpfull in interpreting the variation of the measured e.m.f. with the shift-angle. Their application results in the fact that the third harmonic is the main factor behind the variation in the measured e.m.f. This conclusion is readily noticeable by having a look at Figs. 6, 7 and 8.

For  $\tau = 180^\circ$ , it is seen that the measured e.m.f. on a machine model<sup>2</sup> is approximately constant for all shift-angles. This result completely agrees with the effect of  $H_3$  which is nearly constant. For  $\tau = 120^\circ$ , the same thing could be said about the measured e.m.f. in the d-axis region where the third harmonic effect could be assumed to be abscent. The severe reduction in the induced e.m.f. around the q-axis can be explained with reference to the highest increase of the third harmonic effect around the same axis.

Away from m.m.f. harmonic analysis, a quick prediction can be done by observing the variation in the relative actual area (A), which is defined as

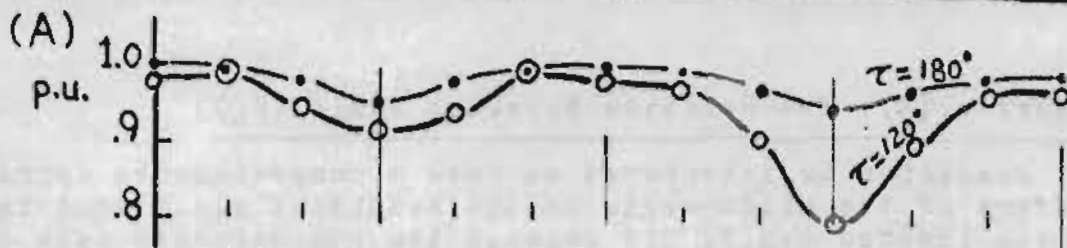


Fig. 5 Relative Actual Area

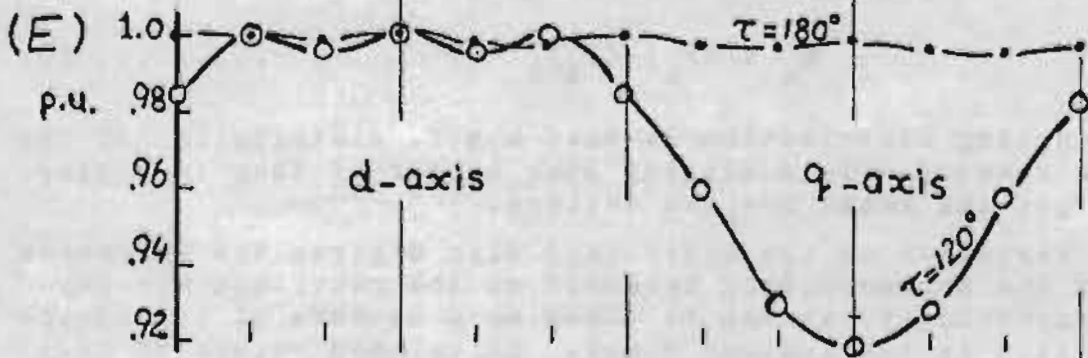


Fig. 6 Measured E.M.F.

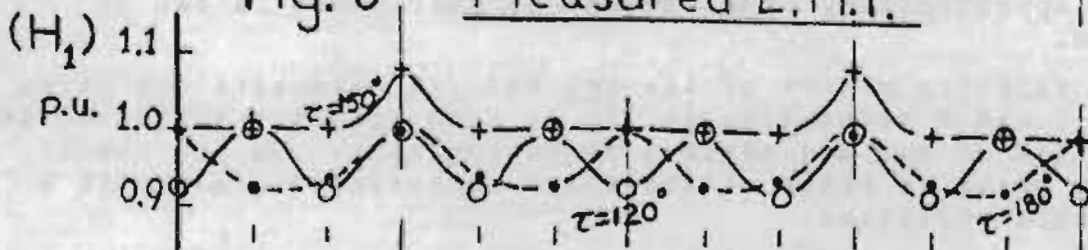


Fig. 7 Relative 1st Harmonic Ratio

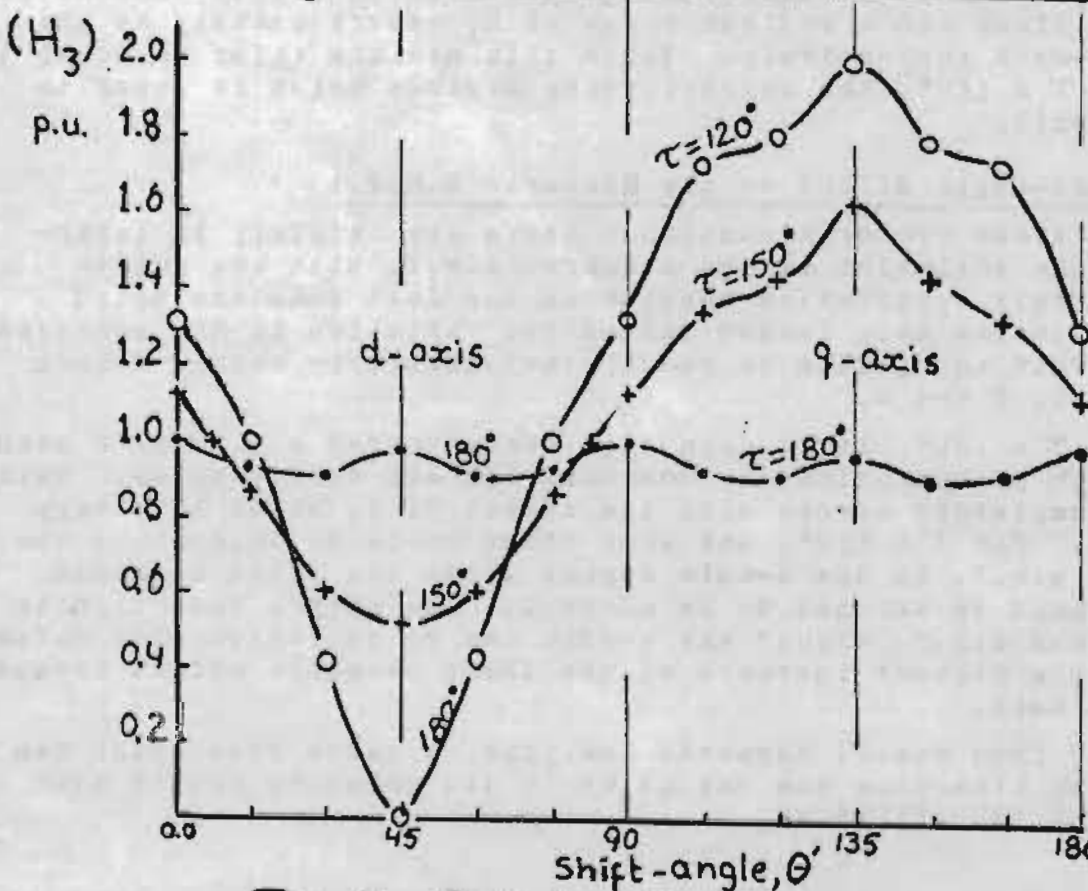


Fig. 8 Relative 3rd Harmonic Ratio

$$A = \frac{\text{half-wave area of the resultant distribution}}{\text{half-wave area of the mono-acting distribution}}$$

$$= (a)/(a)_0 \quad \dots\dots\dots(21)$$

The variation of this ratio with  $\theta'$  (Table (2) and Fig.(5)) shows a relatively agreement with the variation in the measured e.m.f., either for  $\tau = 180^\circ$  or for  $\tau = 120^\circ$ .

## 6. CONCLUSIONS:

The study involves the derivation of two alternative forms of the e.m.f. equation for the idealised d.w.r. synchronous generator. Both equations have the same form of their corresponding ordinary equations derived for synchronous generator with conventional rotor. The equations obtained show that the sinusoidal induced e.m.f. is not affected by shifting the air-gap resultant field.

In order to predict the e.m.f. variation due to shifting the resultant field axis around a real d.w.r., a harmonic analysis study is carried out on the various m.m.f. waveforms. It is found that both criteria "the fundamental peak ratio" and "the ratio of fundamental area" are not enough for predicting the e.m.f. variation with shift-angle. An additional criterion is therefore introduced to enable us to take higher harmonics into consideration.

The study shows that the third harmonic is the main factor behind the e.m.f. variation caused by shifting the resultant field. Accordingly, the variation of the e.m.f. measured on machine model has found its interpretation.

Away from the harmonic analysis a quick prediction of e.m.f. variation, due to shifting the resultant field, can be done by following the variation in the relative actual area of the various m.m.f. waveforms.

## 7. REFERENCES:

1. ABOU-TABL, H.A.: "Divided-Winding-Rotor Synchronous Generator, No-Load Field Control Factors", Bulletin of the Faculty of Engineering, El-Mansoura University, Vol. III, No. 2 December, 1978.
2. ABOU-TABL, H.A.: "Divided-Winding-Rotor Synchronous Generator, Analytical Study of the No-Load Field Distribution", Bulletin of the Faculty of Engineering, El-Mansoura University, Vol. IV, No. 1 June, 1979.
3. ADKINS, B.: "The General Theory of Electrical Machines", Third Printing, Chapman & Hall Ltd, London, 1967.
4. FITZGERALD, A.E., KINGSLEY, C.: "Electric Machinery", 2nd Edition, New York Mc Graw-Hill Book Co., 1965.
5. HANCOCK, N.N.: "Matrix Analysis of Electrical Machines", The Macmillan Co., New York, 1964.